Neurobiology of Aging 34 (2013) 2613–2622

Contents lists available at SciVerse ScienceDirect

Neurobiology of Aging

journal homepage: www.elsevier.com/locate/neuaging

Amyloid beta immunization worsens iron deposits in the choroid plexus and cerebral microbleeds

Nelly Joseph-Mathurin [a,b], Olène Dorieux [a,b,c], Stéphanie G. Trouche [d,e], Allal Boutajangout [f,g,1], Audrey Kraska [a,b,h], Pascaline Fontès [d,e], Jean-Michel Verdier [d,e], Einar M. Sigurdsson [f,g], Nadine Mestre-Francés [d,e], Marc Dhenain [a,b,i,*]

[a] CEA, DSV, I2BM, MIRCen, 18 route du panorama, 92265 Fontenay-aux-Roses cedex, France
[b] CNRS, URA 2210, 18 route du panorama, 92265 Fontenay-aux-Roses cedex, France
[c] CNRS UMR 7179, MNHN, 4 avenue du Petit Château, 91800 Brunoy, France
[d] INSERM U710, Université Montpellier 2, place Eugène Bataillon, 34095 Montpellier cedex 5, France
[e] Ecole Pratique des Hautes Etudes, 46 rue de Lille, 75007 Paris, France
[f] Department of Physiology and Neuroscience, and Psychiatry, MSB459, New York University School of Medicine, 550 First Avenue, New York, NY 10016, USA
[g] Department of Psychiatry, New York University School of Medicine, New York, NY, USA
[h] Institut de Recherche SERVIER, 125 chemin de Ronde, 78290 Croissy-sur-Seine, France
[i] CEA, DSV, I2BM, Neurospin, CEA Saclay, 91191 Gif-sur-Yvette, France

ARTICLE INFO

Article history:
Received 17 September 2012
Received in revised form 20 April 2013
Accepted 16 May 2013
Available online 22 June 2013

Keywords:
Aβ-immunization
Aging
Alzheimer's disease
ARIA (amyloid imaging related abnormalities)
Choroid plexus
Iron
Lemur
Microcebus murinus
Microhemorrhages
MRI
Primate

ABSTRACT

Anti-amyloid beta (Aβ) immunotherapy provides potential benefits in Alzheimer's disease patients. Nevertheless, strategies based on $A\beta_{1-42}$ peptide induced encephalomyelitis and possible microhemorrhages. These outcomes were not expected from studies performed in rodents. It is critical to determine if other animal models better predict side effects of immunotherapies. Mouse lemur primates can develop amyloidosis with aging. Here we used old lemurs to study immunotherapy based on $A\beta_{1-42}$ or Aβ-derivative ($K6A\beta_{1-30}$). We followed anti-$A\beta_{40}$ immunoglobulin G and M responses and Aβ levels in plasma. In vivo magnetic resonance imaging and histology were used to evaluate amyloidosis, neuroinflammation, vasogenic edema, microhemorrhages, and brain iron deposits. The animals responded mainly to the $A\beta_{1-42}$ immunogen. This treatment induced immune response and increased Aβ levels in plasma and also microhemorrhages and iron deposits in the choroid plexus. A complementary study of untreated lemurs showed iron accumulation in the choroid plexus with normal aging. Worsening of iron accumulation is thus a potential side effect of Aβ-immunization at prodromal stages of Alzheimer's disease, and should be monitored in clinical trials.

1. Introduction

Alzheimer's disease (AD) is a neurodegenerative disease that is the most common cause of dementia. Anti-amyloid beta (Aβ) immunotherapies aim to reduce the Aβ lesions that are critical for the pathogenesis of this disease (Hardy and Selkoe, 2002). They can be dissociated into: (1) active immunotherapies during which Aβ or Aβ derivative proteins are injected to activate the immune system and elicit anti-Aβ antibodies; or (2) passive immunotherapies that rely on the administration of anti-Aβ antibodies. The initial evaluation of these therapies in transgenic mouse models of β-amyloidosis, was based on active strategy with $A\beta_{1-42}$ peptides in Freund's adjuvant. The outcome was a reduction of Aβ plaques (Schenk et al., 1999) and a stabilization of cognitive performance in these models (Janus et al., 2000; Morgan et al., 2000). These successes led to a first clinical trial based on administration of synthetic $A\beta_{1-42}$ peptide associated with the QS21 adjuvant (AN1792) in patients with clinical criteria for a diagnosis of AD. This trial decreased Aβ load (Ferrer et al., 2004; Masliah et al., 2005; Nicoll et al., 2003), reduced some but not all (Holmes et al., 2008) of the neuronal alterations that characterize AD (Boche et al., 2010; Serrano-Pozo et al., 2010),

* Corresponding author at: MIRCen, URA CEA CNRS 2210, 18 route du panorama, 92265 Fontenay-aux-Roses cedex, France. Tel.: +33 1 46 54 81 92; fax: +33 1 46 54 84 51.
E-mail address: Marc.Dhenain@cea.fr (M. Dhenain).
[1] Current affiliation: King Abdulaziz University, School of Medicine, Jeddah. Kingdom of Saudi Arabia.

0197-4580/$ – see front matter © 2013 Published by Elsevier Inc.
http://dx.doi.org/10.1016/j.neurobiolaging.2013.05.013

and provided some cognitive benefits in certain patients (Gilman et al., 2005; Hock et al., 2003). However, this first clinical trial induced meningoencephalomyelitis in some individuals (Orgogozo et al., 2003). This alteration was attributed to cytotoxic T cells and/or autoimmune reactions to AN1792. Other possible side effects of immunotherapies such as severe cerebral amyloid angiopathy (CAA) and microhemorrhages have also been reported during this trial (Ferrer et al., 2004; Uro-Coste et al., 2010). Also, in most patients without meningoencephalomyelitis from the AN1792 trial, cognitive outcomes were not modified by the therapy (Holmes et al., 2008). Since this first trial, several clinical trials have been initiated using either active or passive immunotherapies (see Aisen and Vellas, 2013 and Mangialasche et al., 2010 for reviews). They provided interesting results such as a reduction of amyloid load (Rinne et al., 2010), but no significant improvement of cognitive outcomes (Aisen and Vellas, 2013). They also reported side effects such as microhemorrhages and vasogenic edemas (Sperling et al., 2011), although the latter lesion seems to occur mainly during passive immunotherapy and not in active immunotherapy. The side effects that can be detected in vivo using magnetic resonance imaging (MRI) in humans have been called "amyloid imaging-related abnormalities" (Sperling et al., 2011).

After these outcomes, several points became obvious for further trials. First, new trials should be administered in prodromal stages of the disease. Second, approaches based on active immunotherapy should selectively target B-cell epitopes leading to humoral (Th2) immunity and antibody production without stimulating T cells to avoid neuroinflammation and toxicity. This can be done by selecting appropriate adjuvants and vaccines. For example, the alum adjuvant might be better than Freund's adjuvant because it promotes humoral immunity (Asuni et al., 2006; Cribbs et al., 2003). Regarding the vaccines, several developments tried to reduce or eliminate the midregion and C-terminal part of Aβ because it contains T-cell epitopes and retains the 2 major immunogenic sites of Aβ peptides (i.e., the 1–11 and 22–28 residues) (Cribbs et al., 2003; Jameson and Wolf, 1988). For example, some approaches were based on the use of the $A\beta_{1-6}$ (Wiessner et al., 2011), $A\beta_{1-15}$ (Ghochikyan et al., 2006; Muhs et al., 2007), $A\beta_{1-15}$ derivatives (Maier et al., 2006), $A\beta_{1-16}$ (Muhs et al., 2007), or $A\beta_{1-28}$ (Petrushina et al., 2008) peptides. In a previous work, we designed the $K6A\beta_{1-30}$, a nonfibrillogenic, nontoxic Aβ homologous peptide which has 6 lysines on the N-terminus to increase immunogenicity and enhance solubility. This modification, in addition to removal of the C-terminal amino acids of Aβ, also reduces its propensity to form β-sheets. This immunogen elicited an antibody response similar to $A\beta_{1-42}$ in mice which resulted in a comparable therapeutic efficacy (Sigurdsson et al., 2001). Third, outcomes of the first trial also highlighted the need to test anti-Aβ vaccines in non-transgenic animal models to better predict their efficiency and potential side effects. For example, Lemere et al. (2004) and Gandy et al. (2004) evaluated immunotherapy with $A\beta_{1-42}$ in Freund's adjuvant in old Caribbean Vervets and Rhesus Macaques, respectively. They showed that immunized primates generated anti-Aβ antibodies. Plasmatic Aβ levels were elevated in the immunized animals although, unlike control animals, they had no plaque deposition in the brain.

Here, we investigated immunotherapy based on $A\beta_{1-42}$ or Aβ-derivatives administered with alum adjuvant in old mouse lemurs. In this small primate (100 g), 5% to 20% of aged animals develop Aβ amyloidosis (Languille et al., 2012; Mestre-Frances et al., 2000). A previous study in young animals, comparing $A\beta_{1-42}$ and Aβ-derivatives, has shown that immunization promotes antibody response against $A\beta_{1-40}$ and $A\beta_{1-42}$ and increases plasmatic Aβ load (Trouche et al., 2009). Here, we studied animals without amyloid plaques or with a very small extracellular amyloid load, but presenting with intracellular and vascular amyloid deposits. We show that $A\beta_{1-42}$ immunization increases plasmatic Aβ levels, and also microhemorrhages and iron deposition in the choroid plexus (CP) of aged animals including in Aβ-plaque free animals. The latter effect is a new potential side effect of anti-Aβ treatment administered at the prodromal stage of the disease.

2. Methods

2.1. Animals

Our study evaluated the effects of immunotherapy and aging in mouse lemurs. First, the immunotherapy study was performed in 20 animals aged 4.1 to 6.4 years: a first cohort of 8 animals (5.9 ± 0.1 years) were treated with $A\beta_{1-42}$ ($n = 4$) or with $K6A\beta_{1-30}$ ($n = 4$) vaccines and were followed-up using MRI and biochemical parameters (antibody titers, Aβ levels in plasma) during 10 months (Fig. 1); a second cohort of 12 animals (4.7 ± 0.2 years) were followed with the same protocol but treated with $K6A\beta_{1-30}$ ($n = 6$) or with the adjuvant alone ($n = 6$). The brains of these 20 animals were then histologically evaluated. Second, the aging study was performed in 28 non-treated mouse lemurs aged 1.6 to 6.4 years (young adults, $n = 9$; 1.9 ± 0.2 years; middle-aged, $n = 11$; 4.5 ± 0.1 years; and old, $n = 8$; 5.9 ± 0.1 years) that were studied using MRI in vivo. All the animals were born and raised in a laboratory breeding colony at Montpellier, France. Animal care was in accordance with institutional guidelines and the animal protocol was approved by the local ethics committee (authorization #CEEA-LR-1002).

2.2. Peptides

The peptides used for the immunization were synthesized using the solid-phase technique at the Keck Foundation at Yale University, as previously described in Asuni et al. (2006) and Sigurdsson et al. (2004).

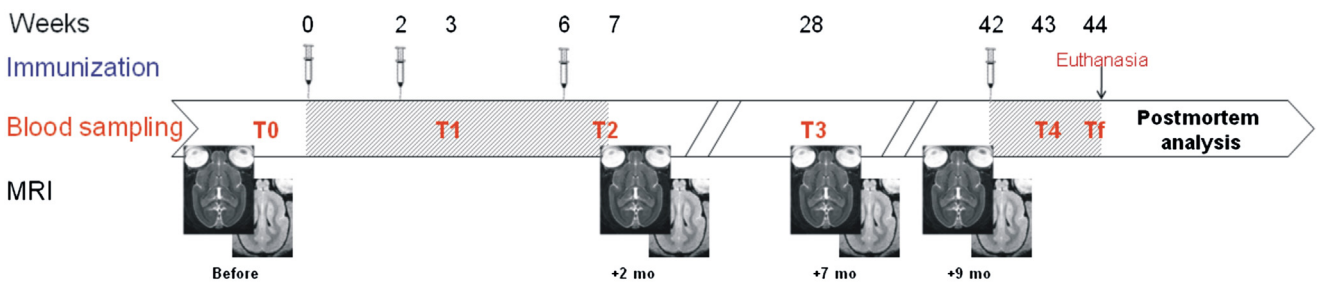

Fig. 1. Diagram depicting the timeline of the immunizations, bleeds for measurements of antibody response and amyloid beta levels, and magnetic resonance imaging sessions. Hatched areas correspond to immunization and second phase of immunization.

2.3. Injections and bleeds

Animals vaccinated with $A\beta_{1-42}$ received $A\beta_{1-42}$ in alum adjuvant (100-μL subcutaneous injections; Alhydrogel; Brenntag Biosector, Frederiksund, Denmark). Animals vaccinated with $K6A\beta_{1-30}$ received $K6A\beta_{1-30}$ in alum adjuvant (100-μL subcutaneous injections; Adju-Phos; Brenntag Biosector). Alum adjuvant was chosen because it is the most common adjuvant in human vaccines (Gupta, 1998) and because it promotes Th2 immunity (Asuni et al., 2006). In the context of the vaccine, aluminium is used at low dose that should not be toxic for the organism, and that is why it is approved for clinical use in humans. Animals treated with the alum adjuvant alone received Adju-Phos (100-μL subcutaneous injections; Brenntag Biosector). $A\beta_{1-42}$ and $K6A\beta_{1-30}$ peptides were mixed with the alum adjuvant at a concentration of 1 mg/mL and the solution was rotated overnight at 4 °C before administration to allow the peptide to adsorb onto the aluminum particles, which have an opposite charge to the peptide.

The animals received 4 injections. The second, third, and fourth injection were administered 2, 6, and 42 weeks after the first injection (Fig. 1). The primates were bled before the first immunization (T0), and 1 week after the second (T1; 3 weeks) and third injection (T2; 7 weeks). T3 was at 28 weeks (22 weeks after the third injection). T4 and Tf were performed at 43 and 44 weeks, respectively (1 week and 2 weeks after the fourth injection, respectively). The Tf was performed at the time of euthanasia of the animal. The mouse lemurs went through several MRI sessions, before, and 2, 7, and 9 months after the injections (Fig. 1).

2.4. Antibody levels

Anti-$A\beta_{1-40}$ and anti-$K6A\beta_{1-30}$ immunoglobulin (Ig) M and IgG antibodies were evaluated from the plasma of mouse lemurs. IgM antibodies are usually produced immediately after an exposure to antigens, and IgG antibodies are associated with a later response. Anti-$A\beta_{1-40}$ and anti-$K6A\beta_{1-30}$ antibody levels were determined at 1:200 dilution of plasma using an enzyme-linked immunosorbent assay as described previously (Asuni et al., 2006; Sigurdsson et al., 2001), in which the full-length $A\beta_{1-40}$ or $K6A\beta_{1-30}$ peptides were coated onto microtiter wells (Immulon 2 HB; ThermoScientific, Waltham, MA, USA). Antibody levels were detected using an anti-primate IgG and IgM linked to a horseradish peroxidase (Alpha Diagnostics; San Antonio, TX, USA) (Trouche et al., 2009).

2.5. $A\beta_{1-40}$ levels in plasma

For the measurement of free $A\beta_{1-40}$ in plasma, a 10% dilution of untreated plasma was used, and the detection was performed using an enzyme-linked immunosorbent assay kit (Biosource, Camarillo, CA, USA) as previously described (Trouche et al., 2009). $A\beta_{1-42}$ levels in plasma were below the limit of detection.

2.6. MRI acquisition and image processing

T2-weighted (T2w) and T2*-weighted (T2*w) images were recorded on a 7-Tesla spectrometer (Bruker Pharmascan) with an isotropic resolution of 234 μm. The T2w sequence (Repetition time TR/ echo time TE = 2500/69.2 ms, inversion time TI = 60 ms, rapid acquisition with relaxation enhancement RARE factor = 12) was used to evaluate cerebral inflammation (hyperintense signal). The T2*w sequence (Repetition time TR/echo time TE = 40/8 ms, flip angle = 12°) was used to evaluate iron deposits and microhemorrhages (hypointense signal).

Four MRI sessions (before, and 2, 7, and 9 months after the beginning of immunization; Fig. 1) were performed for the longitudinal follow-up of the vaccinated primates. Animals were preanesthetized with a subcutaneous injection of atropine (0.025 mg/kg). Twenty minutes later, they were anesthetized using isoflurane (5% for induction and 1% during the MRI scans as described in Dhenain et al., 2003). Respiration rate and body temperature were monitored to ensure stability of the animal; body temperature was maintained stable with a water-heated bed and air-heated ventilation.

On T2w images, cerebral inflammation can be detected as hyperintense regions. Such signal alterations were evaluated by visual inspection. On T2*w images, iron deposits and microhemorrhages led to a hypointense signal and cerebrospinal fluid accumulation within the ventricles led to hyperintense signals. Voxels with hypointense signals were quantified using the following method (Anatomist-freeware, http://brainvisa.info/): first, a threshold ($T = M \times 0.5$) was calculated for each image by using the mean intensity (M) of a cortical region of the image and a constant coefficient of 0.5. The cortical region was selected with constant landmarks in the parietal cortex and was exempt of hypointense voxels. Voxels with signal intensity below the calculated threshold were considered hypointense. These voxels were painted using a graphic tablet. They were classified as belonging to the CP or brain parenchyma on the basis of their anatomical location (Bons et al., 1998). The volumes of hypointense voxels belonging to the CP or brain parenchyma (index of cerebral microhemorrhages) were then automatically calculated by the image analysis freeware.

2.7. Histology

The animals were euthanized with an overdose of ketamine (approximately 0.03 mL/100 g). Their brains were postfixed with 4% paraformaldehyde in 0.1 M phosphate buffer (pH 7.4) at 4 °C. The mouse lemur hemibrains were embedded in paraplast (MM France, Francheville, France) and cut into 6-μm serial sagittal sections and used for iron staining and immunohistochemistry.

2.7.1. Iron staining

Microhemorrhages and other iron deposits were analyzed using Perls' staining which reveals ferric ions. Sagittal brain sections were incubated in a solution composed of 5% potassium ferrocyanide and 10% hydrochloric acid (vol/vol) for 30 minutes and rinsed in distilled water. Subsequently, nuclear fast red (0.1%) counterstain was performed, and the sections were rinsed again in distilled water. After dehydration, sections were coverslipped with Mountex (Histolab, Gothenburg, Sweden).

2.7.2. Immunohistochemistry

Sagittal brain sections were stained for amyloid. Amyloid detection was based on $A\beta_{1-42}$ rabbit polyclonal (FCA3542; Calbiochem, Merck, Darmstadt, Germany) that binds to the C-terminus of the $A\beta_{1-42}$ peptide, and 4G8 monoclonal antibody (Covance, Emeryville, CA, USA) that recognizes the middle region (amino acid residues 17–24) of Aβ. FCA3542 is specific for Aβ, ending at residue 42 and does not stain Amyloid Precursor Protein (Barelli et al., 1997). A pretreatment with formic acid for 15 minutes was used for $A\beta_{1-42}$ and 4G8 staining. Endogenous peroxidase was quenched by treating the sections with distilled water containing 1% H_2O_2 for 30 minutes at room temperature. Sections were blocked in 3% goat serum. Products were diluted in Tris-buffered saline, pH 7.6. Primary antibodies were diluted at 1:1000. Slices were incubated with secondary biotinylated antibodies (anti-rabbit and anti-mouse antibodies for $A\beta_{1-42}$ and 4G8, respectively) for 30 minutes at room temperature. Next the signal was amplified by using avidin-peroxidase complex standard (ABC-kit, Vectastain; Vector Laboratories, Burlingame, CA, USA). Final reaction used 3,3′-diaminobenzidine tetrahydrochloride (Vector Laboratories) as a chromogen for peroxidase activity. All

washing steps (3 times for 3 minutes each) and antibody dilution were done using Tris-buffered saline, pH 7.6. Incubation with the ABC complex and detection with 3,3′-diaminobenzidine tetrahydrochloride were done according to the manufacturer's manual. Hematoxylin counterstaining was performed according to a standard procedure. After dehydration, sections were coverslipped with Mountex.

2.7.3. Quantification of histological sections

Histological sections were analyzed using a Leitz Laborlux S (Leica Microsystems, Nanterre, France), using the Mercator software (Mercator Pro, Rev 7.9.8; ExploraNova, La Rochelle, France). This software permits quantification of histological sections and can generate maps of counted objects such as extracellular $A\beta_{1-42}$ deposits (12 sagittal brain sections per animal), intracellular 4G8 positive objects (30 sagittal brain sections per animal) or microhemorrhages (7 sagittal brain sections separated by 300 μm per animal). Counting was performed on each section per cortical area (frontal, parietal, and occipital) for the intracellular 4G8-positive deposits (fields of $500 \times 500\ \mu m^2$) or on whole brain sections for microhemorrhages. A global semiquantitative evaluation of vessels stained by $A\beta_{1-42}$ was also performed. The following scoring scale was used based on the number of Aβ stained vessels per slide: (0) zero-, (+) 1–3-, (++) 4–6-, and (+++) more than 6 Aβ-stained vessels detected per slide (Table 1).

2.8. Statistical analysis

Data were analyzed using Statistica 7.1 (Statsoft France, Maisons-Alfort, France). Microhemorrhages and intracellular Aβ were analyzed using the Student *t* test. Antibody level, plasmatic Aβ, and volume of hypointense regions were analyzed using repeated measures analysis of variance and Fisher's least significant difference (LSD) test for post hoc analysis. The conditions required to use parametric statistical tests (normality, homoscedasticity, sphericity of the data) were respected. Correlative studies were based on nonparametric Spearman rank correlation.

3. Results

3.1. $A\beta_{1-42}$ immunization modulates immune responses and plasmatic amyloid levels

Before immunization, the animals from the cohorts (treated with $A\beta_{1-42}$, $K6A\beta_{1-30}$, or adjuvant alone) had similar low levels of anti-$A\beta_{1-40}$ IgG and IgM antibodies (Fig. 2A and C) or anti-$K6A\beta_{1-30}$ IgG and IgM antibodies (data not shown). They also had similar plasma levels of $A\beta_{1-40}$ (Fig. 2E and F).

In the $A\beta_{1-42}$ vaccine group, the anti-$A\beta_{1-40}$ antibody titers were highly increased at T1, T2, T4, and Tf after immunization, compared with their levels before immunization (respectively 17-, 15-, 12-, and 14-fold for IgG levels and 8-, 5-, 3-, and 4-fold for the IgM levels; all $p < 0.01$). Anti-$K6A\beta_{1-30}$ antibody titers of the $A\beta_{1-42}$ vaccine group were also increased, compared with their levels before immunization (at T1 and Tf for IgG and T1, T4, and Tf for IgM; all $p < 0.05$). In this group, plasma levels of $A\beta_{1-40}$ were also increased, in particular during the first immunization phase (T1 approximately a 465% increase; $p < 0.005$), T2 approximately a 108% increase (nonsignificant [ns]), T4 approximately a 48% increase (ns), and Tf approximately 32% increase (ns). The increased levels of $A\beta_{1-40}$ in plasma paralleled within the same time frame the increased levels of anti-$A\beta_{1-40}$ IgG and IgM. These data suggest that the $A\beta_{1-42}$ group responded to immunization.

In the $K6A\beta_{1-30}$ groups, the anti-$A\beta_{1-40}$ IgG and IgM antibody titers were low and not significantly modified at any time point after immunization, compared with their levels before immunization (all $p > 0.05$; see Fig. 2A and C for the first cohort and Fig. 2B and D for the second cohort). The animals vaccinated with $A\beta_{1-42}$ had thus higher anti-$A\beta_{1-40}$ IgG and IgM levels compared with the animals treated with $K6A\beta_{1-30}$ (respectively, $F(1,3) = 23$; $p < 0.05$ and $F(1,3) = 182$; $p < 0.001$). Also, the anti-$K6A\beta_{1-30}$ IgG or IgM antibody titers from animals treated with $K6A\beta_{1-30}$ vaccine were not modified at any time after the immunization, compared with their levels before immunization (all $p > 0.05$, blood analysis performed on the first cohort). Plasma levels of $A\beta_{1-40}$ were also not significantly altered in the $K6A\beta_{1-30}$ groups, compared with their levels before immunization (Fig. 2E and F). Thus, the $A\beta_{1-42}$ group presented higher $A\beta_{1-40}$ levels in plasma, compared with the $K6A\beta_{1-30}$ group ($F(1,3) = 100$; $p < 0.005$; Fig. 2E).

In the adjuvant group, the anti-$A\beta_{1-40}$ IgG and IgM levels and the plasma levels of $A\beta_{1-40}$ were not modified, compared with their levels before immunization (all $p > 0.05$; Fig. 2B, D, and F).

Because of the lack of immune response and Aβ modulation in plasma in the $K6A\beta_{1-30}$ groups and the similar lack of response in the $K6A\beta_{1-30}$ and adjuvant groups, the animals treated with $K6A\beta_{1-30}$ vaccine in the first cohort were considered non-responders during our study. Note that for ethical reasons and because we had strong arguments showing that $K6A\beta_{1-30}$ vaccine did not induce a significant immune response, an additional group of adjuvant animals, age-matched to the groups of the first cohort ($A\beta_{1-42}$ vs. $K6A\beta_{1-30}$), was not used in the current study.

Table 1
Semiquantitative evaluation of vascular Aβ in the different animals

Animal	Vaccine group	Vascular Aβ (score)
184	$A\beta_{1-42}$	+
189	$A\beta_{1-42}$	+
192	$A\beta_{1-42}$	+
194	$A\beta_{1-42}$	+
190	$K6A\beta_{1-30}$	++
191	$K6A\beta_{1-30}$	+
193	$K6A\beta_{1-30}$	+++
195	$K6A\beta_{1-30}$	+++

Score scale: few (+), moderate (++), high (+++).
Key: Aβ, amyloid beta.

3.2. $A\beta_{1-42}$ and its derivative do not induce meningoencephalitis or vasogenic edema

All the animals involved in the current study were followed longitudinally using in vivo MRI. None of the animals displayed hyperintense T2w magnetic resonance (MR) signals that might suggest vasogenic edema or neuroinflammatory processes (Fig. 3).

3.3. $A\beta_{1-42}$ vaccine worsens age-associated iron accumulation in the CP

T2*w images revealed hypointense signals in the ventricles of old animals, before and during immunization (Fig. 4A, B, and E). Quantification revealed an increased size of these hypointense signals in animals treated with the $A\beta_{1-42}$ vaccine compared with the $K6A\beta_{1-30}$ group ($F_{\text{vaccine by session}}(2,10) = 5$; $p < 0.05$; Fig. 4C). Such signal changes on MR images are characteristic of iron deposition. Histological analysis confirmed that the hypointense regions detected on MRI corresponded to iron accumulation in epithelial cells of the CP (Fig. 4G). Hypointense signal changes were not detected in the second cohort ($K6A\beta_{1-30}$ vs. adjuvant) ($F_{\text{vaccine by session}}(2,20) = 0.03$; ns).

To further evaluate iron accumulation in the CP, T2*w MRI scans were recorded in a cohort of young adults ($n = 9$; 1.9 ± 0.2 years) and middle-aged animals ($n = 11$; 4.5 ± 0.1 years). MRI scans from these young and middle-aged animals were

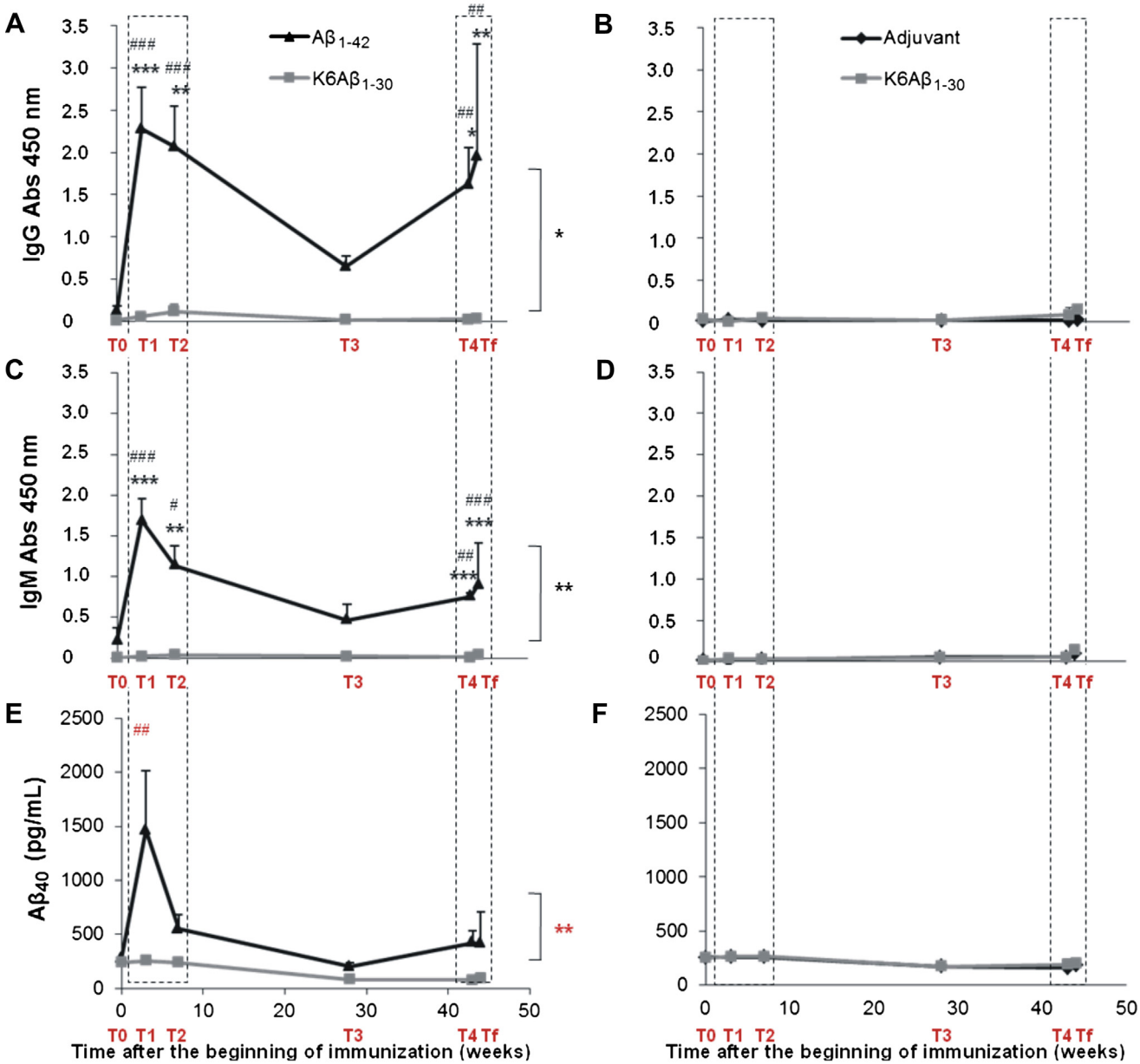

Fig. 2. Anti-amyloid beta $(A\beta)_{1-40}$ immunoglobulin (Ig) G and IgM antibody responses and plasma $A\beta_{1-40}$ in the mouse lemurs treated with $A\beta_{1-42}$, $K6A\beta_{1-30}$, and adjuvant. The $A\beta_{1-42}$ vaccinated lemurs (black triangles) developed more anti-$A\beta_{1-40}$ IgG (A) and IgM (C) compared with the $K6A\beta_{1-30}$ group (gray square) ($F_{\text{IgG vaccine effect}}(1,3) = 23$; $^{*}\ p < 0.05$ and $F_{\text{IgM vaccine effect}}(1,3) = 182$; $^{**}\ p < 0.001$) during immunization phases (dotted line frames). The $K6A\beta_{1-30}$-vaccinated lemurs (gray squares) did not develop more anti-$A\beta_{1-40}$ IgG (B) and IgM (D) compared with the adjuvant group (black rhomb) (nonsignificant [ns]). (A) IgG responses were higher in the $A\beta_{1-42}$ group (post hoc analyses at $T1_{K6A\beta1-30\text{ vs. }A\beta1-42}$, $^{***}\ p < 0.0001$; $T2_{K6A\beta1-30\text{ vs. }A\beta1-42}$, $^{**}\ p < 0.005$; $T4_{K6A\beta1-30\text{ vs. }A\beta1-42}$, $^{*}\ p < 0.01$; $Tf_{K6A\beta1-30\text{ vs. }A\beta1-42}$, $^{**}\ p < 0.005$). Their values were significantly increased compared with their basal levels (post hoc analyses, $IgG_{T0\text{ vs. }T1}$, $^{###}\ p < 0.0005$; $IgG_{T0\text{ vs. }T2}$, $^{###}\ p < 0.0005$; $IgG_{T0\text{ vs. }T4}$, $^{##}\ p < 0.005$; $IgG_{T0\text{ vs. }Tf}$, $^{##}\ p < 0.005$). (C) IgM responses were higher in the $A\beta_{1-42}$ group (post hoc analyses at $T1_{K6A\beta1-30\text{ vs. }A\beta1-42}$, $^{***}\ p < 0.000001$; $T2_{K6A\beta1-30\text{ vs. }A\beta1-42}$, $^{**}\ p < 0.005$; $T4_{K6A\beta1-30\text{ vs. }A\beta1-42}$, $^{***}\ p < 0.0005$; $Tf_{K6A\beta1-30\text{ vs. }A\beta1-42}$, $^{***}\ p < 0.0005$). Their values were significantly increased compared with their basal levels (post hoc analyses $IgM_{T0\text{ vs. }T1}$, $^{###}\ p < 0.0005$; $IgM_{T0\text{ vs. }T2}$, $^{#}\ p < 0.01$; $IgM_{T0\text{ vs. }T4}$, $^{##}\ p < 0.005$; $IgM_{T0\text{ vs. }Tf}$, $^{###}\ p < 0.0005$). The plasmatic $A\beta_{1-40}$ was modulated following the profile of immune responses in the animals vaccinated with $A\beta_{1-42}$ (E) but no modulation in the animal vaccinated with $K6A\beta_{1-30}$ compared with adjuvant (F). The lemurs vaccinated with $A\beta_{1-42}$ (black triangle) had an increased plasmatic $A\beta_{1-40}$ compared with the $K6A\beta_{1-30}$ group (gray square) ($F_{\text{plasm}A\beta1-40\text{ vaccine effect}}(1,3) = 100$; $^{**}\ p < 0.005$). In this group, the increase in plasma $A\beta_{1-40}$ levels was particularly high at T1 during the first immunization phase (post hoc analysis, $^{##}\ p < 0.005$) and had subsided at T2 (ns). Reimmunization did not lead to as robust of an anti-$A\beta_{1-40}$ antibody response at T4 and Tf (ns). In the other group, $K6A\beta_{1-30}$ was not immunogenic and the level of $A\beta_{1-40}$ in the plasma did not change (ns). Statistics are indicated on the right side of the graph for a global vaccine effect according to analysis of variance, and above the curves for post hoc analyses. Statistical annotations: asterisks represent the significant differences between the groups (*, **, or ***); sharps represent the significant differences between T0 and other time points after immunization (#, ##, or ###). *, # $p < 0.05$; **, ##, $p < 0.005$; ***, ###, $p < 0.0005$. Abbreviation: Abs, absorbance.

compared with MRI scans from the old animals ($n = 8$; 5.9 ± 0.1 years) of the first cohort before immunization. In vivo T2*w MRI of the young animals did not show any hypointense signal at the level of the CP (Fig. 4D and F). The size of the hypointense signal at the level of the CP increased in the middle-aged compared with young animals and further increased in old mouse lemurs ($F(2,25) = 8$; $p < 0.005$; post hoc analyses, $p < 0.05$; Fig. 4H).

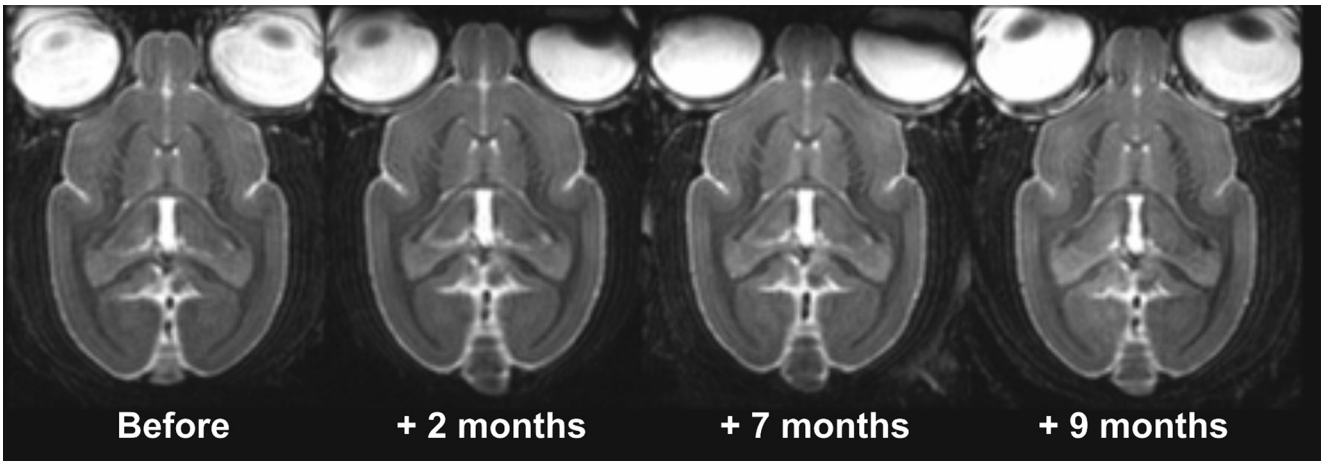

Fig. 3. Assessment of vasogenic edema or neuroinflammation on magnetic resonance imaging (MRI) scans before and during amyloid beta immunization. MRI scans do not highlight hyperintense signal characteristics of vasogenic edema or neuroinflammation on T2-weighted images, irrespective of the MRI session or the vaccine group. The hyperintense signal visible on these images corresponds to cerebrospinal fluid.

3.4. $A\beta_{1-42}$ vaccine increases microhemorrhages

Histological studies revealed microhemorrhages (<10 μm) in the cortex (Fig. 5A) and other brain regions (globus pallidus, thalamus [Fig. 5B], subthalamic regions, ventral hippocampus, amygdala). The subcortical microhemorrhages were more numerous than the cortical microhemorrhages. The $A\beta_{1-42}$ group had more parenchymal microhemorrhages, compared with the $K6A\beta_{1-30}$ group ($t(6) = 2.72$; $p < 0.05$; Fig. 5C). The number of microhemorrhages was correlated with the anti-$A\beta_{1-40}$ IgG response and plasma $A\beta_{1-40}$ levels at the late stages of immunization (mean values for T0, T4 and Tf, $p < 0.005$ and T4 and Tf, $p < 0.005$, respectively). No significant difference of number of microhemorrhages could be detected in the second cohort ($K6A\beta_{1-30}$ vs. adjuvant; data not shown).

The microhemorrhages detected on histological sections could, however, not be detected (as hypointense spots) on in vivo MRI, which can be explained by their small size.

3.5. Neuropathological evaluation of vascular, intracellular, and extracellular amyloidosis

Aβ deposits were detected in the vasculature of several animals (Fig. 6A). The $A\beta_{1-42}$ responders had fewer vascular Aβ deposits compared with the $K6A\beta_{1-30}$ animals (Table 1). These Aβ deposits

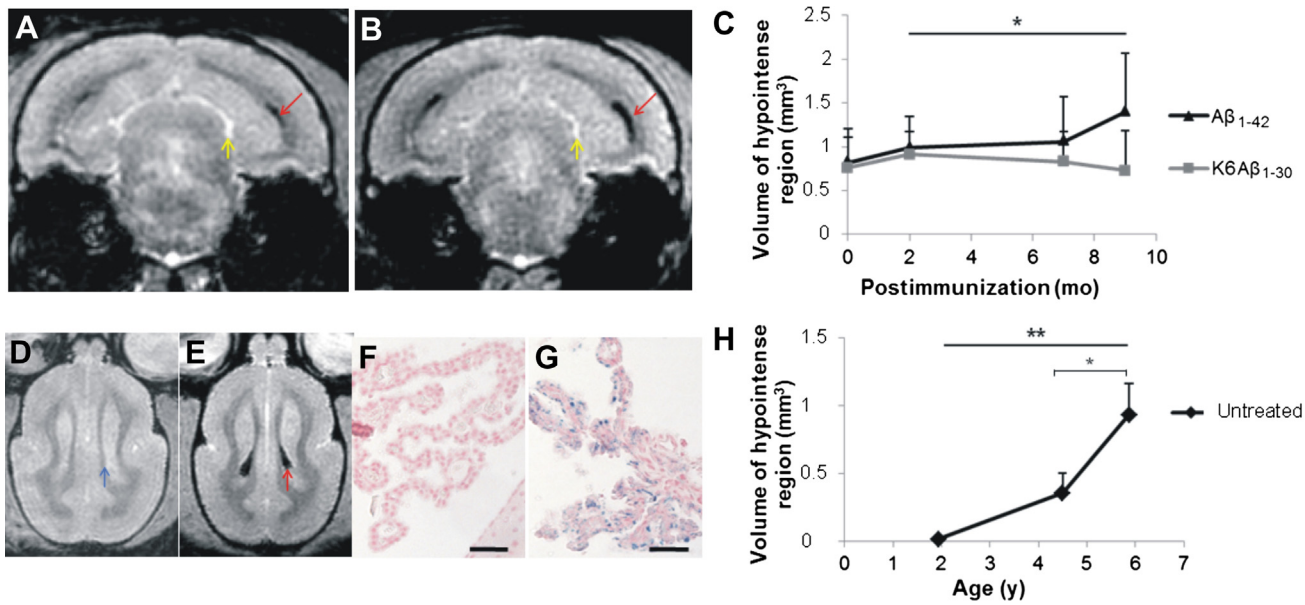

Fig. 4. Iron deposition in the choroid plexus of mouse lemurs. Effects of amyloid beta (Aβ) immunization and age. The T2-weighted images show hypointense signals (red arrows), characteristic of iron deposition, distributed inside the ventricles of the old animals. On these images, cerebrospinal fluid appears with a hyperintense signal (yellow arrows). The hypointense signal was increased in the same animal after 9 months of vaccination with $A\beta_{1-42}$ vaccine (B), compared with before immunization (A). (C) The volume of hypointense signal increased in old lemurs vaccinated with $A\beta_{1-42}$ (black triangles) compared with animals vaccinated with $K6A\beta_{1-30}$ (gray squares) (analysis of variance, $F_{\text{vaccine*time effect}}(2,10) = 5$; * $p < 0.05$). The volume of hypointense signals did not change in the animals from the second cohort ($K6A\beta_{1-30}$ vs. adjuvant; data not shown). Comparison of young and old naive animals. Hypointense signal corresponding to iron in the choroid plexus was observed in old (E, red arrow; and G, blue stain on Perls' stained sections) but not in young animals (D) and (F). In these latter samples, iron-free choroid plexus had the same intensity as surrounding tissue (blue arrow). (H) The analysis of young (1.9 ± 0.2), middle-aged (4.5 ± 0.1), and old (5.9 ± 0.1) lemurs showed an age-associated increased of the volume of hypointense regions characteristic of iron deposits in the choroid plexus (analysis of variance, $F(2,25) = 8$; ** $p < 0.005$ and post hoc analyses comparing middle-aged vs. old, $t(25) = 2$; * $p < 0.05$). Scale bars, 50 μm.

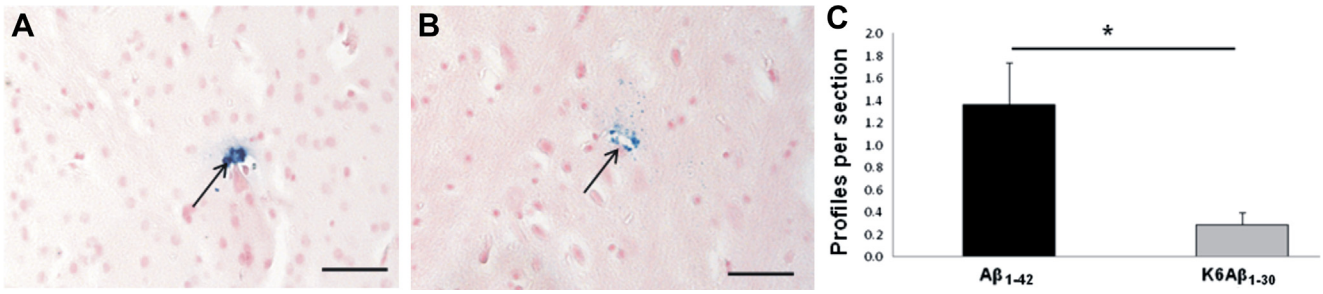

Fig. 5. Microhemorrhages in the brain parenchyma of the lemurs after 10 months of vaccination. Example of Perls'-positive microhemorrhages located in the occipital cortex (A, arrow) and thalamus (B, arrow). (C) More microhemorrhages were detected in the old lemurs vaccinated with $A\beta_{1-42}$ (black) compared with the $K6A\beta_{1-30}$ group (gray) ($t(6) = 2.72$; * $p < 0.05$). Scale bars, 50 μm.

were never detected in the vicinity of microhemorrhages. Aβ immunoreactivity was also detected in the epithelial cells of the CP (Fig. 6B) but was not colocalized with the iron deposits. However, no obvious difference between animals from the $A\beta_{1-42}$, $K6A\beta_{1-30}$ or adjuvant groups could be detected by visual inspection.

Intracellular Aβ immunoreactivity was also detected in neurons of the frontal, parietal, and occipital cortical regions and in the hippocampus from $A\beta_{1-42}$-, $K6A\beta_{1-30}$-, or adjuvant-treated primates (Fig. 6C and E). In the 2 cohorts, the degree of 4G8 positive objects was similar, irrespective of the region and experimental group (Fig. 6G).

It is noteworthy that extracellular Aβ deposits were only detected in 2 animals of the study that were treated with $K6A\beta_{1-30}$. The deposits were diffuse and restricted to the subiculum in 1 animal and were rare and localized in several cortical regions (frontal, parietal) and in the subiculum in the second animal (Fig. 6F).

4. Discussion

The current study evaluated Aβ immunization in aged mouse lemur primates, an animal that has the same Aβ sequence as humans and can spontaneously develop intracellular, extracellular, and vascular Aβ deposits with age (Bons et al., 1994; Kraska et al., 2011; Languille et al., 2012). In mouse lemur primates, the Aβ load is much lower than in transgenic mouse models of amyloidosis that overexpress mutated forms of human amyloid precursor protein (APP). The latter models have a very high Aβ load and are largely used to evaluate various immunotherapy protocols. In mouse lemurs, only a small proportion of aged animals (5%–20%) naturally develop extracellular Aβ plaques (Languille et al., 2012; Mestre-Frances et al., 2000). In our 2 cohorts of 8 and 12 aged lemurs we could thus expect that 1 or 2 animals had extracellular Aβ plaques before immunization or were in the process of developing such plaques. Our immunohistological study on 20 animals revealed amyloid plaques in only 2 animals (10% of animals). This value is consistent with the prevalence of amyloid plaques in lemurs even without treatment. We can thus consider that the number of animals presenting with plaques in the treated population was not strongly reduced compared with the number of animals presenting with plaques in the general population. All of the aged animals, however, had intracellular Aβ immunoreactivity and Aβ in plasma. It seems that the Aβ plaque load in lemurs mimics normal aging in humans (i.e., a situation with low Aβ plaque load). Results from our study might thus be predictive of the consequence of Aβ immunotherapy in normal aged non-AD humans.

We showed that active immunization with the full-length $A\beta_{1-42}$, but not with a derivative, $K6A\beta_{1-30}$, elicits an immune response in our cohort of old mouse lemurs. This immune response was associated with increased $A\beta_{1-40}$ levels in the plasma. Because the antibodies generated by the immunization process bound at least some Aβ in the blood, we can speculate that our measured plasma levels of Aβ were underestimated compared with the real Aβ load in the plasma. In addition, in the animals treated with $A\beta_{1-42}$, we observed increased levels of microhemorrhages and an increased accumulation of iron in the CP. No sign of

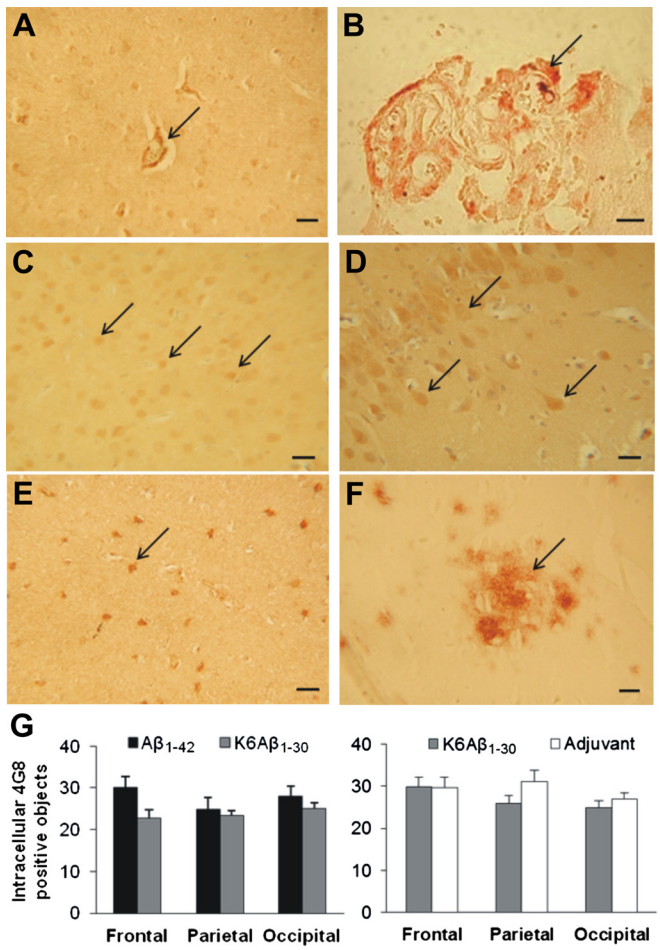

Fig. 6. Amyloidosis in vaccinated mouse lemurs. Amyloid beta (Aβ) immunoreactivity was detected in the vessels (A; 4G8, arrow) and choroid plexus (B; 4G8, arrow) of vaccinated animals. Intracellular Aβ was observed in various brain regions such as the frontal cortex (C; $A\beta_{1-42}$ staining [FCA3542], arrows), the hippocampus (D; $A\beta_{1-42}$ staining [FCA3542], arrows) or the parietal cortex (E; 4G8, arrow). Two of the immunized lemurs had extracellular diffuse Aβ plaques (F; 4G8, arrow). (G) Quantification of the intracellular staining (4G8 staining) in the frontal, parietal, and occipital cortices revealed no significant differences between the 2 groups whatever the cohort ($A\beta_{1-42}$ [black] vs. $K6A\beta_{1-30}$ [gray], or adjuvant [dark gray] vs. $K6A\beta_{1-30}$ [gray]). Scale bars, 25 μm.

meningoencephalomyelitis or vasogenic edema could be detected in the vaccinated animals. In humans, during passive immunotherapies based on monoclonal antibodies, the presence of microhemorrhages is a risk factor for developing vasogenic edema, but other risk factors such as the apolipoprotein E4 status are also associated with the risk of vasogenic edema (Sperling et al., 2011). Vasogenic edemas are, however, not reported during active immunotherapies such as ours (Sperling et al., 2011). The lack of vasogenic edema in our study is thus consistent with studies in humans. Meningoencephalomyelitis is the major side effect reported in active immunotherapies (Orgogozo et al., 2003). The mechanisms associated with the occurrence of microhemorrhages and meningoencephalomyelitis are, however, different. Microhemorrhages are expected to be associated with redistribution of Aβ into cerebral blood vessels (Wilcock et al., 2004) or with binding of antibodies to existing CAA (Racke et al., 2005), and meningoencephalomyelitis is related to the hyperactivation of T cells, a process that was minimized in the design of our immunotherapy trial by using alum adjuvant that promotes Th2 immunity (Asuni et al., 2006). In our study, the lack of meningoencephalomyelitis despite the presence of microhemorrhages is thus consistent with the expected lack of T-cell hyperactivation with our vaccine.

In the present study, the response to the K6Aβ_{1-30} vaccine was much lower than that induced by the Aβ_{1-42} vaccine and was similar to that induced by the adjuvant. In our previous study in young animals, both Aβ_{1-42} and K6Aβ_{1-30} immunotherapies administered with alum adjuvants were associated with a robust antibody response and increased level of Aβ_{1-40} in plasma (Trouche et al., 2009). Of these 2, Aβ_{1-42} elicited a stronger immune response against Aβ as expected. In another previous study we also showed a high antibody response toward K6Aβ_{1-30} in old lemurs (Mestre-Frances et al., 2010), an outcome that is converse to the result from the current study. These apparently opposite results are explained by the lower immunogenicity of the K6Aβ_{1-30}, compared with Aβ_{1-42}, which leads to more variable responses in different cohorts of old animals because antibody response generally subsides with aging. This lower immunogenicity of K6Aβ_{1-30} is, however, of interest because it indicates that K6Aβ_{1-30} is potentially safer than Aβ_{1-42}. K6Aβ_{1-30} might thus be a good treatment to initiate in middle-aged subjects. It is also interesting that the variable response to K6Aβ_{1-30} has also been reported in transgenic mice, where a cohort of 11 to 24-month-old mice were shown to respond to treatment with K6Aβ_{1-30} and 19 to 24-month-old animals did not respond (Asuni et al., 2006).

The Aβ_{1-42} responder animals presented a transient IgM response and a long-lasting higher IgG response. The transient plasma Aβ increase paralleled the IgG and IgM responses within the same time frame. A possible explanation is that immunization led to a clearance of Aβ from the brain via a peripheral sink process (DeMattos et al., 2001; Lemere et al., 2003). However, the extracellular aggregated Aβ load is small in lemurs and we did not find any difference of extracellular Aβ or intracellular 4G8-positive object load in the 2 groups of treated animals. Another possible explanation for the high Aβ level in plasma is that immunoglobulins sequestered Aβ and increased its half-life (Levites et al., 2006).

Our study highlighted that vaccination with an Aβ_{1-42} vaccine increases iron accumulation in the epithelial cells of the CP. To our knowledge, this is the first study showing a link between iron deposits in CP and Aβ immunotherapy. It has been shown that epithelial cells of the CP are involved in iron exchanges between the blood and the brain (Deane et al., 2004). Moreover, it has been proposed that the CP plays a role in the modulation of iron metabolism in aging and AD (Mesquita et al., 2012). Also, peripheral inflammation is known to modulate expression of choroidal genes implicated in the immune response cascade, in barrier integrity (Marques et al., 2009b), and iron homeostasis (Marques et al., 2009a). The presumed inflammation induced by immunotherapy might thus modulate the function of the CP and lead to increased iron accumulation in the CP.

To date, in humans, iron accumulation in the CP has never been reported after Aβ immunotherapy. However, during pathological conditions, iron accumulates in the CP of humans (Kira et al., 2000), which is reminiscent of the increase in iron that we detected in the CP of lemurs. Because of these similarities, we suggest that iron accumulation in the CP might also occur during Aβ immunotherapy in humans. This potential effect should be further evaluated in MR images of anti−Aβ-immunized human subjects, because MRI does detect iron accumulation in human CP (Kira et al., 2000).

In parallel, in mouse lemurs we found, in a small cohort of animals, that Aβ_{1-42} treatment increases microhemorrhages, despite the lack of extracellular Aβ plaques and the low level of vascular Aβ in the brain. In a previous study based on postmortem MRI, we already showed that aged lemurs can spontaneously develop microhemorrhages during normal aging (Bertrand et al., 2013). We confirmed this in this study, and also showed that the number of microhemorrhages is relatively low in control animals (0.29 ± 0.10 profiles per section). The microhemorrhage load found in our study was comparable with data reported in transgenic mouse models of AD (see, e.g., a 0.5 profile per section in Wilcock et al., 2004). However, the number of microhemorrhages in our treated animals (1.36 ± 0.38 profiles per section) was lower than those reported in transgenic mice (3.4 profiles per section in Wilcock et al., 2004). This can be related to a different treatment, but also probably to the lower global amyloid load in lemurs compared with transgenic mice. In most studies in transgenic mice, microhemorrhages have been associated with an increased level of vascular amyloidosis (Thakker et al., 2009; Wang et al., 2011; Wilcock et al., 2004, 2007). From these studies it has been suggested that vascular amyloidosis is a prerequisite for Aβ-immunization-associated microhemorrhages. However, data from a preventative study in mice showed that Aβ immunization at an early stage increases microbleeds without increasing CAA (Schroeter et al., 2008). Our data in primates are consistent with this latter study and suggest that vascular Aβ deposits are not mandatory to induce microhemorrhages after Aβ immunization. One possible explanation is that T-cell response induced by the epitopes such as 16 to 24 and 34 to 42 of Aβ occurred in mouse lemurs even if the adjuvant was designed to minimize this response. This T cell response could induce microbleeds in the absence of vascular Aβ deposits.

To conclude, we have evaluated Aβ immunization in the mouse lemur, a primate model of normal aging or prodromal stage of AD with minimal extracellular Aβ deposition. We have shown that even in the absence of severe β-amyloidosis, Aβ-immunization can lead to iron deposition in the CP and microhemorrhages. This study suggests that Aβ immunization of normal aged subjects or of aged patients at a very early stage of AD can induce side effects that might have clinical relevance. This should be taken into account in the design of future clinical evaluations in patients at a very early AD stage.

Disclosure statement

All authors have no conflicts of interest.

Animal care was in accordance with institutional guidelines and the animal protocol was approved by the local ethics committee (authorization #CEEA-LR-1002).

Acknowledgements

This work was supported by the France-Alzheimer association; the longevity program from the CNRS; the Regional Council of

Martinique; the National Foundation for Alzheimer's Disease and Related Disorders; and the National Institute on Aging (R01-AG020197). O.D. was financed by Hoffmann-La Roche.

References

Aisen, P.S., Vellas, B., 2013. Editorial: passive immunotherapy for Alzheimer's disease: what have we learned, and where are we headed? J. Nutr. Health Aging 17, 49–50.

Asuni, A.A., Boutajangout, A., Scholtzova, H., Knudsen, E., Li, Y.S., Quartermain, D., Frangione, B., Wisniewski, T., Sigurdsson, E.M., 2006. Vaccination of Alzheimer's model mice with Abeta derivative in alum adjuvant reduces Abeta burden without microhemorrhages. Eur. J. Neurosci. 24, 2530–2542.

Barelli, H., Lebeau, A., Vizzavona, J., Delaere, P., Chevallier, N., Drouot, C., Marambaud, P., Ancolio, K., Buxbaum, J.D., Khorkova, O., Heroux, J., Sahasrabudhe, S., Martinez, J., Warter, J.M., Mohr, M., Checler, F., 1997. Characterisation of new polyclonal specific for 40 and 42 amino acid-long amyloid ß peptides: their use to examine the cell biology of presenilins and the immunochemistry of sporadic Alzheimer's disease and cerebral amyloid angiopathy cases. Mol. Med. 3, 695–707.

Bertrand, A., Pasquier, A., Petiet, A., Wiggins, C., Kraska, A., Joseph-Mathurin, N., Aujard, F., Mestre-Francés, N., Dhenain, M., 2013. Micro-MRI study of cerebral aging: detection of hippocampal subfield reorganization, microhemorrhages, and amyloid plaques in mouse lemur primates. Plos One 8, e56593.

Boche, D., Donald, J., Love, S., Harris, S., Neal, J.W., Holmes, C., Nicoll, J.A., 2010. Reduction of aggregated Tau in neuronal processes but not in the cell bodies after Abeta42 immunisation in Alzheimer's disease. Acta Neuropathol. 120, 13–20.

Bons, N., Mestre, N., Ritchie, K., Petter, A., Podlisny, M., Selkoe, D., 1994. Identification of amyloid beta protein in the brain of the small, short-lived lemurian primate *Microcebus murinus*. Neurobiol. Aging 15, 215–220.

Bons, N., Sihol, S., Barbier, V., Mestre-Frances, N., Albe-Fessard, D., 1998. A stereotaxic atlas of the grey lesser mouse lemur brain (*Microcebus murinus*). Brain Res. Bull. 46, 1–173.

Cribbs, D.H., Ghochikyan, A., Vasilevko, V., Tran, M., Petrushina, I., Sadzikava, N., Babikyan, D., Kesslak, P., Kieber-Emmons, T., Cotman, C.W., Agadjanyan, M.G., 2003. Adjuvant-dependent modulation of Th1 and Th2 responses to immunization with beta-amyloid. Intern. Immunol. 15, 505–514.

Deane, R., Zheng, W., Zlokovic, B.V., 2004. Brain capillary endothelium and choroid plexus epithelium regulate transport of transferrin-bound and free iron into the rat brain. J. Neurochem. 88, 813–820.

DeMattos, R.B., Bales, K.R., Cummins, D.J., Dodart, J.C., Paul, S.M., Holtzman, D.M., 2001. Peripheral anti-A beta antibody alters CNS and plasma A beta clearance and decreases brain A beta burden in a mouse model of Alzheimer's disease. Proc. Natl. Acad. Sci. U.S.A. 98, 8850–8855.

Dhenain, M., Chenu, E., Hisley, C.K., Aujard, F., Volk, A., 2003. Regional atrophy in the brain of lissencephalic mouse lemur primates: measurement by automatic histogram-based segmentation of MR images. Magn. Res. Med. 50, 984–992.

Ferrer, I., Boada Rovira, M., Sanchez Guerra, M.L., Rey, M.J., Costa-Jussa, F., 2004. Neuropathology and pathogenesis of encephalitis following amyloid-beta immunization in Alzheimer's disease. Brain Pathol. 14, 11–20.

Gandy, S., DeMattos, R.B., Lemere, C.A., Heppner, F.L., Leverone, J., Aguzzi, A., Ershler, W.B., Dai, J., Fraser, P., Hyslop, P.S., Holtzman, D.M., Walker, L.C., Keller, E.T., 2004. Alzheimer A beta vaccination of rhesus monkeys (*Macaca mulatta*). Alzheimer Dis. Assoc. Disord. 18, 44–46.

Ghochikyan, A., Mkrtichyan, M., Petrushina, I., Movsesyan, N., Karapetyan, A., Cribbs, D.H., Agadjanyan, M.G., 2006. Prototype Alzheimer's disease epitope vaccine induced strong Th2-type anti-Abeta antibody response with Alum to Quil A adjuvant switch. Vaccine 24, 2275–2282.

Gilman, S., Koller, M., Black, R.S., Jenkins, L., Griffith, S.G., Fox, N.C., Eisner, L., Kirby, L., Rovira, M.B., Forette, F., Orgogozo, J.M., (QS-21)-201 Study Team, 2005. Clinical effects of Abeta immunization (AN1792) in patients with AD in an interrupted trial. Neurology 64, 1553–1562.

Gupta, R.K., 1998. Aluminum compounds as vaccine adjuvants. Adv. Drug Deliv. Rev. 32, 155–172.

Hardy, J., Selkoe, D.J., 2002. The amyloid hypothesis of Alzheimer's disease: progress and problems on the road to therapeutics. Science 297, 353–356.

Hock, C., Konietzko, U., Streffer, J.R., Tracy, J., Signorell, A., Muller-Tillmanns, B., Lemke, U., Henke, K., Moritz, E., Garcia, E., Wollmer, M.A., Umbricht, D., de Quervain, D.J., Hofmann, M., Maddalena, A., Papassotiropoulos, A., Nitsch, R.M., 2003. Antibodies against beta-amyloid slow cognitive decline in Alzheimer's disease. Neuron 38, 547–554.

Holmes, C., Boche, D., Wilkinson, D., Yadegarfar, G., Hopkins, V., Bayer, A., Jones, R.W., Bullock, R., Love, S., Neal, J.W., Zotova, E., Nicoll, J.A., 2008. Long-term effects of Abeta42 immunisation in Alzheimer's disease: follow-up of a randomised, placebo-controlled phase I trial. Lancet 372, 216–223.

Jameson, B.A., Wolf, H., 1988. The antigenic index: a novel algorithm for predicting antigenic determinants. Comput. Appl. Biosci. 4, 181–186.

Janus, C., Pearson, J., McLaurin, J., Mathews, P.M., Jiang, Y., Schmidt, S.D., Chishti, M.A., Horne, P., Heslin, D., French, J., Mount, H.T., Nixon, R.A., Mercken, M., Bergeron, C., Fraser, P.E., St George-Hyslop, P., Westaway, D., 2000. A beta peptide immunization reduces behavioural impairment and plaques in a model of Alzheimer's disease. Nature 408, 979–982.

Kira, R., Ohga, S., Takada, H., Gondo, K., Mihara, F., Hara, T., 2000. MR choroid plexus sign of iron overload. Neurology 55, 1340.

Kraska, A., Dorieux, O., Picq, J.L., Petit, F., Bourrin, E., Chenu, E., Volk, A., Perret, M., Hantraye, P., Mestre-Frances, N., Aujard, F., Dhenain, M., 2011. Age associated cerebral atrophy in mouse lemur primates. Neurobiol. Aging 32, 894–906.

Languille, S., Blanc, S., Blin, O., Canale, C.I., Dal-Pan, A., Devau, G., Dhenain, M., Dorieux, O., Epelbaum, J., Gomez, D., Hardy, I., Henry, P.Y., Irving, E.A., Marchal, J., Mestre-Francés, N., Perret, M., Picq, J.L., Pifferi, F., Rahman, A., Schenker, E., Terrien, J., Théry, M., Verdier, J.M., Aujard, F., 2012. The grey mouse lemur: a non-human primate model for ageing studies. Ageing Res. Rev. 11, 150–162.

Lemere, C.A., Beierschmitt, A., Iglesias, M., Spooner, E.T., Bloom, J.K., Leverone, J.F., Zheng, J.B., Seabrook, T.J., Louard, D., Li, D., Selkoe, D.J., Palmour, R.M., Ervin, F.R., 2004. Alzheimer's disease abeta vaccine reduces central nervous system abeta levels in a non-human primate, the Caribbean vervet. Am. J. Pathol. 165, 283–297.

Lemere, C.A., Spooner, E.T., LaFrancois, J., Malester, B., Mori, C., Leverone, J.F., Matsuoka, Y., Taylor, J.W., DeMattos, R.B., Holtzman, D.M., Clements, J.D., Selkoe, D.J., Duff, K.E., 2003. Evidence for peripheral clearance of cerebral Abeta protein following chronic, active Abeta immunization in PSAPP mice. Neurobiol. Dis. 14, 10–18.

Levites, Y., Smithson, L.A., Price, R.W., Dakin, R.S., Yuan, B., Sierks, M.R., Kim, J., McGowan, E., Reed, D.K., Rosenberry, T.L., Das, P., Golde, T.E., 2006. Insights into the mechanisms of action of anti-Abeta antibodies in Alzheimer's disease mouse models. FASEB J. 20, 2576–2578.

Maier, M., Seabrook, T.J., Lazo, N.D., Jiang, L., Das, P., Janus, C., Lemere, C.A., 2006. Short amyloid-beta (Abeta) immunogens reduce cerebral Abeta load and learning deficits in an Alzheimer's disease mouse model in the absence of an Abeta-specific cellular immune response. J. Neurosci. 26, 4717–4728.

Mangialasche, F., Solomon, A., Winblad, B., Mecocci, P., Kivipelto, M., 2010. Alzheimer's disease: clinical trials and drug development. Lancet Neurol. 9, 702–716.

Marques, F., Falcao, A.M., Sousa, J.C., Coppola, G., Geschwind, D., Sousa, N., Correia-Neves, M., Palha, J.A., 2009a. Altered iron metabolism is part of the choroid plexus response to peripheral inflammation. Endocrinology 150, 2822–2828.

Marques, F., Sousa, J.C., Coppola, G., Geschwind, D.H., Sousa, N., Palha, J.A., Correia-Neves, M., 2009b. The choroid plexus response to a repeated peripheral inflammatory stimulus. BMC Neurosci. 10, 135.

Masliah, E., Hansen, L., Adame, A., Crews, L., Bard, F., Lee, C., Seubert, P., Games, D., Kirby, L., Schenk, D., 2005. Abeta vaccination effects on plaque pathology in the absence of encephalitis in Alzheimer disease. Neurology 64, 129–131.

Mesquita, S.D., Ferreira, A.C., Sousa, J.C., Santos, N.C., Correia-Neves, M., Sousa, N., Palha, J.A., Marques, F., 2012. Modulation of iron metabolism in aging and in Alzheimer's disease: relevance of the choroid plexus. Front. Cell. Neurosci. 6, 25.

Mestre-Frances, N., Keller, E., Calenda, A., Barelli, H., Checler, F., Bons, N., 2000. Immunohistochemical analysis of cerebral cortical and vascular lesions in the primate *Microcebus murinus* reveal distinct amyloid beta 1-42 and beta 1-40 immunoreactivity profiles. Neurobiol. Dis. 7, 1–8.

Mestre-Frances, N., Trouche, S., Boutajangout, A., Asuni, A.A., Arribat, Y., Rouland, S., Wisniewski, T., Frangione, B., Maurice, T., Sigurdsson, E.M., Verdier, J.M., 2010. Abeta derivative vaccination in old mouse lemur primates. Alzheimers Dement. 6, S223.

Morgan, D., Diamond, D.M., Gottschall, P.E., Ugen, K.E., Dickey, C., Hardy, J., Duff, K., Jantzen, P., DiCarlo, G., Wilcock, D., Connor, K., Hatcher, J., Hope, C., Gordon, M., Arendash, G.W., 2000. A beta peptide vaccination prevents memory loss in an animal model of Alzheimer's disease. Nature 408, 982–985.

Muhs, A., Hickman, D.T., Pihlgren, M., Chuard, N., Giriens, V., Meerschman, C., van der Auwera, I., van Leuven, F., Sugawara, M., Weingertner, M.C., Bechinger, B., Greferath, R., Kolonko, N., Nagel-Steger, L., Riesner, D., Brady, R.O., Pfeifer, A., Nicolau, C., 2007. Liposomal vaccines with conformation-specific amyloid peptide antigens define immune response and efficacy in APP transgenic mice. Proc. Natl. Acad. Sci. U.S.A. 104, 9810–9815.

Nicoll, J.A., Wilkinson, D., Holmes, C., Steart, P., Markham, H., Weller, R.O., 2003. Neuropathology of human Alzheimer disease after immunization with amyloid-beta peptide: a case report. Nat. Med. 9, 448–452.

Orgogozo, J.M., Gilman, S., Dartigues, J.F., Laurent, B., Puel, M., Kirby, L.C., Jouanny, P., Dubois, B., Eisner, L., Flitman, S., Michel, B.F., Boada, M., Frank, A., Hock, C., 2003. Subacute meningoencephalitis in a subset of patients with AD after Abeta42 immunization. Neurology 61, 46–54.

Petrushina, I., Ghochikyan, A., Mkrtichyan, M., Mamikonyan, G., Movsesyan, N., Ajdari, R., Vasilevko, V., Karapetyan, A., Lees, A., Agadjanyan, M.G., Cribbs, D.H., 2008. Mannan-Abeta28 conjugate prevents Abeta-plaque deposition, but increases microhemorrhages in the brains of vaccinated Tg2576 (APPsw) mice. J. Neuroinflammation 5, 42.

Racke, M.M., Boone, L.I., Hepburn, D.L., Parsadainian, M., Bryan, M.T., Ness, D.K., Piroozi, K.S., Jordan, W.H., Brown, D.D., Hoffman, W.P., Holtzman, D.M., Bales, K.R., Gitter, B.D., May, P.C., Paul, S.M., DeMattos, R.B., 2005. Exacerbation of cerebral amyloid angiopathy-associated microhemorrhage in amyloid precursor protein transgenic mice by immunotherapy is dependent on antibody recognition of deposited forms of amyloid beta. J. Neurosci. 25, 629–636.

Rinne, J.O., Brooks, D.J., Rossor, M.N., Fox, N.C., Bullock, R., Klunk, W.E., Mathis, C.A., Blennow, K., Barakos, J., Okello, A.A., Rodriguez Martinez de Liano, S., Liu, E., Koller, M., Gregg, K.M., Schenk, D., Black, R., Grundman, M., 2010. 11C-PiB PET assessment of change in fibrillar amyloid-beta load in patients with Alzheimer's disease treated with bapineuzumab: a phase 2, double-blind, placebo-controlled, ascending-dose study. Lancet Neurol. 9, 363–372.

Schenk, D., Barbour, R., Dunn, W., Gordon, G., Grajeda, H., Guido, T., Hu, K., Huang, J., Johnson-Wood, K., Khan, K., Kholodenko, D., Lee, M., Liao, Z., Lieberburg, I., Motter, R., Mutter, L., Soriano, F., Shopp, G., Vasquez, N., Vandevert, C., Walker, S., Wogulis, M., Yednock, T., Games, D., Seubert, P., 1999. Immunization with amyloid-beta attenuates Alzheimer-disease-like pathology in the PDAPP mouse. Nature 400, 173–177.

Schroeter, S., Khan, K., Barbour, R., Doan, M., Chen, M., Guido, T., Gill, D., Basi, G., Schenk, D., Seubert, P., Games, D., 2008. Immunotherapy reduces vascular amyloid-beta in PDAPP mice. J. Neurosci. 28, 6787–6793.

Serrano-Pozo, A., William, C.M., Ferrer, I., Uro-Coste, E., Delisle, M.B., Maurage, C.A., Hock, C., Nitsch, R.M., Masliah, E., Growdon, J.H., Frosch, M.P., Hyman, B.T., 2010. Beneficial effect of human anti-amyloid-beta active immunization on neurite morphology and tau pathology. Brain 133, 1312–1327.

Sigurdsson, E.M., Knudsen, E., Asuni, A., Fitzer-Attas, C., Sage, D., Quartermain, D., Goni, F., Frangione, B., Wisniewski, T., 2004. An attenuated immune response is sufficient to enhance cognition in an Alzheimer's disease mouse model immunized with amyloid-beta derivatives. J. Neurosci. 24, 6277–6282.

Sigurdsson, E.M., Scholtzova, H., Mehta, P.D., Frangione, B., Wisniewski, T., 2001. Immunization with a nontoxic/nonfibrillar amyloid-beta homologous peptide reduces Alzheimer's disease-associated pathology in transgenic mice. Am. J. Pathol. 159, 439–447.

Sperling, R.A., Jack Jr., C.R., Black, S.E., Frosch, M.P., Greenberg, S.M., Hyman, B.T., Scheltens, P., Carrillo, M.C., Thies, W., Bednar, M.M., Black, R.S., Brashear, H.R., Grundman, M., Siemers, E.R., Feldman, H.H., Schindler, R.J., 2011. Amyloid-related imaging abnormalities in amyloid-modifying therapeutic trials: recommendations from the Alzheimer's Association Research Roundtable Workgroup. Alzheimers Dement. 7, 367–385.

Thakker, D.R., Weatherspoon, M.R., Harrison, J., Keene, T.E., Lane, D.S., Kaemmerer, W.F., Stewart, G.R., Shafer, L.L., 2009. Intracerebroventricular amyloid-beta antibodies reduce cerebral amyloid angiopathy and associated microhemorrhages in aged Tg2576 mice. Proc. Natl. Acad. Sci. U.S.A. 106, 4501–4506.

Trouche, S.G., Asuni, A., Rouland, S., Wisniewski, T., Frangione, B., Verdier, J.M., Sigurdsson, E.M., Mestre-Francés, N., 2009. Antibody response and plasma Abeta1-40 levels in young *Microcebus murinus* primates immunized with Abeta1-42 and its derivatives. Vaccine 27, 957–964.

Uro-Coste, E., Russano de Paiva, G., Guilbeau-Frugier, C., Sastre, N., Ousset, P.J., da Silva, N.A., Lavialle-Guillotreau, V., Vellas, B., Delisle, M.B., 2010. Cerebral amyloid angiopathy and microhemorrhages after amyloid beta vaccination: case report and brief review. Clin. Neuropathol. 29, 209–216.

Wang, A., Das, P., Switzer 3rd, R.C., Golde, T.E., Jankowsky, J.L., 2011. Robust amyloid clearance in a mouse model of Alzheimer's disease provides novel insights into the mechanism of amyloid-beta immunotherapy. J. Neurosci. 31, 4124–4136.

Wiessner, C., Wiederhold, K.H., Tissot, A.C., Frey, P., Danner, S., Jacobson, L.H., Jennings, G.T., Luond, R., Ortmann, R., Reichwald, J., Zurini, M., Mir, A., Bachmann, M.F., Staufenbiel, M., 2011. The second-generation active Abeta immunotherapy CAD106 reduces amyloid accumulation in APP transgenic mice while minimizing potential side effects. J. Neurosci. 31, 9323–9331.

Wilcock, D.M., Jantzen, P.T., Li, Q., Morgan, D., Gordon, M.N., 2007. Amyloid-beta vaccination, but not nitro-nonsteroidal anti-inflammatory drug treatment, increases vascular amyloid and microhemorrhage while both reduce parenchymal amyloid. Neuroscience 144, 950–960.

Wilcock, D.M., Rojiani, A., Rosenthal, A., Subbarao, S., Freeman, M.J., Gordon, M.N., Morgan, D., 2004. Passive immunotherapy against Abeta in aged APP-transgenic mice reverses cognitive deficits and depletes parenchymal amyloid deposits in spite of increased vascular amyloid and microhemorrhage. J. Neuroinflammation 1, 24.